Space Sci Rev (2008) 137: 149–173
DOI 10.1007/s11214-008-9339-y

Cosmic Ray Induced Ion Production in the Atmosphere

G.A. Bazilevskaya · I.G. Usoskin · E.O. Flückiger · R.G. Harrison · L. Desorgher · R. Bütikofer · M.B. Krainev · V.S. Makhmutov · Y.I. Stozhkov · A.K. Svirzhevskaya · N.S. Svirzhevsky · G.A. Kovaltsov

Received: 23 November 2007 / Accepted: 4 March 2008 / Published online: 22 March 2008

Abstract An overview is presented of basic results and recent developments in the field of cosmic ray induced ionisation in the atmosphere, including a general introduction to the mechanism of cosmic ray induced ion production. We summarize the results of direct and indirect measurements of the atmospheric ionisation with special emphasis to long-term variations. Models describing the ion production in the atmosphere are also overviewed together with detailed results of the full Monte-Carlo simulation of a cosmic ray induced atmospheric cascade. Finally, conclusions are drawn on the present state and further perspectives of measuring and modeling cosmic ray induced ionisation in the terrestrial atmosphere.

Keywords Atmosphere · Ionisation · Cosmic rays

1 Introduction

Cosmic rays are energetic particles of extra-terrestrial origin, which impinge upon the Earth's atmosphere. The galactic cosmic rays (CRs) are charged particles (comprising

G.A. Bazilevskaya (✉) · M.B. Krainev · V.S. Makhmutov · Y.I. Stozhkov · A.K. Svirzhevskaya · N.S. Svirzhevsky
Lebedev Physical Institute Russian Academy of Sciences, Leninsky Prospect, 53, Moscow 119991, Russia
e-mail: bazilevs@fian.fiandns.mipt.ru

I.G. Usoskin
Sodankylä Geophysical Observatory, University of Oulu, P.O. Box 3000, Oulu, Finland
e-mail: ilya.usoskin@oulu.fi

E.O. Flückiger · L. Desorgher · R. Bütikofer
Physikalisches Institut, University of Bern, Sidlerstrasse 5, 3012 Bern, Switzerland

R.G. Harrison
University of Reading, Earley Gate, P.O. Box 243, Reading RG6 6BB, UK

G.A. Kovaltsov
Ioffe Physical-Technical Institute, St. Petersburg 194021, Russia

mostly protons, ∼10% He nuclei and ∼1% other elements; electrons comprise ∼1%) with energies from about 1 MeV (1 MeV = $1.6 \cdot 10^{-13}$ J) up to at least $5 \cdot 10^{13}$ MeV (8 J) (Grieder 2001; Dorman 2004). Low-energy particles are just absorbed in the atmosphere, but those with energies above some 1000 MeV generate new particles through interactions with atomic nuclei in air. Energetic cosmic rays initiate nuclear-electromagnetic cascades in the atmosphere, causing a maximum in secondary particle intensity at the altitude of 15–26 km depending on latitude and solar activity level, the so-called Pfotzer maximum (Bazilevskaya and Svirzhevskaya 1998). The galactic CRs arrive at the Earth constantly but their intensity is modulated by the 11-year cycle of solar activity with the opposite phase i.e. the higher solar activity, the lower the intensity of galactic CRs. Solar CRs (also called solar energetic particles, SEP) are particles accelerated during the explosive energy release at the Sun and by acceleration processes in the interplanetary space (Lario and Simnett 2004). They intrude into the atmosphere sporadically, with a higher probability during periods of high solar activity. Due to their steep energy spectrum, only a small fraction of SEPs with energy around several GeV generates cascades in the atmosphere sufficiently to allow neutron monitors to record a so-called ground-level enhancement, GLE (Miroshnichenko 2004). Another energetic particle population is that of magnetospheric electrons which can precipitate into the atmosphere. They are absorbed in the upper atmosphere, but the X-rays produced by these electrons can penetrate down to the altitude of about 20 km. Electron precipitation occurs more often during the declining phase of the 11-year solar cycle.

The geomagnetic field determines which particles arrive at the Earth at different latitudes, i.e. the geomagnetic field acts as a charged particle discriminator. Motion of a charged particle in the geomagnetic field depends on the particle rigidity $R = c\,P/z\,e$, where c is the speed of light, P and z are the particle momentum and ionic charge number respectively and e is the elementary charge. Particles with equal rigidities move in a similar way in a given magnetic field. Roughly speaking, each geomagnetic latitude may be characterised by a cutoff rigidity, R_c, such that particles with less rigidity cannot arrive at this latitude (Cooke et al. 1991). Low-energy particles can therefore only arrive at high latitudes. Only particles with $R > 15$ GV (kinetic energy > 14 GeV) are able to reach equatorial regions.

In the course of last decades CRs have attracted growing attention as a major source of atmospheric ionisation. This is because CRs are the most important contributor to ion-pair production from ∼3–4 km up to about 50 km. Ions are involved in many atmospheric processes. In particular numerous studies suggest that ionisation due to CR may affect different climate parameters such as cloud cover (Pudovkin and Veretenenko 1995; Svensmark and Friis-Christensen 1997; Feynman and Ruzmaikin 1999; Marsh and Svensmark 2000; Pallé et al. 2004; Usoskin et al. 2004b; Harrison and Stephenson 2006; Usoskin et al. 2006; Voiculescu et al. 2006), precipitation (Stozhkov et al. 1996; Kniveton and Todd 2001; Stozhkov 2003; Kniveton 2004), cyclogenesis in mid- to high-latitude regions (Tinsley et al. 1989; Tinsley and Deen 1991; Pudovkin and Veretenenko 1996; Veretenenko and Thejll 2004), atmospheric transparency (Roldugin and Vashenyuk 1994; Veretenenko and Pudovkin 1997; Roldugin and Tinsley 2004), aerosol formation (Shumilov et al. 1996; Mironova and Pudovkin 2005; Kazil et al. 2006). Some investigations offer possible mechanisms responsible for the observed phenomena, such as the effect of the cosmic ray induced ionisation (CRII) on the global electric circuit (Tinsley and Zhou 2006; Tinsley et al. 2007) or ion-induced nucleation (Svensmark et al. 2007). However, despite extensive theoretical and phenomenological studies, detailed physical mechanisms connecting CRs with the climate parameters remain not fully understood. Thus, it is crucially important to increase the level of understanding of the CR-related changes in the atmospheric ionisation via both systematic and improved measurements and reliable modeling.

2 Measurements of Ionisation in the Atmosphere

2.1 Measurements of Ionisation in the Lower Atmosphere

Although direct measurements of CRs were not made until the twentieth century, early observations of atmospheric electricity measured CRs indirectly, through determining the electrical properties of air. From the late eighteenth century it was known that an electric field continually existed in the fair weather atmosphere, and air had a finite electrical conductivity (Harrison 2004). If there is no appreciable contribution from surface sources of radioactivity, the electrical conductivity arises from the small ions produced by CRs.

2.1.1 Air Conductivity in the Troposphere

The electrical conductivity of aerosol-free air in the troposphere is related to the number concentration of small ions (cluster ions) contained. The total conductivity, σ, is given by

$$\sigma = e(\mu_+ n_+ + \mu_- n_-), \tag{1}$$

where n_+ and n_- are the positive and negative small ion number concentrations respectively, and μ_+ and μ_- are the positive and negative ion mobilities. An important factor in determining the ion concentration is the volumetric ion production rate, q, which, away from the continental surface, is dominated by CR ion production. In aerosol-free air, the mean ion concentration n is given by

$$n = \sqrt{q/\alpha}, \tag{2}$$

where α is the ion-ion recombination rate, which, for cluster ions in surface air, is typically $1.6 \cdot 10^{-6}$ cm^3 sec^{-1} (Chalmers 1967). In polluted air, containing Z aerosol particles per unit volume, n is given by

$$n = \frac{q}{\beta Z}, \tag{3}$$

where β is the ion-aerosol attachment rate. Both Z and β are local properties of the air concerned, however α generally has an approximately constant value.

Clean air therefore provides the simplest case for retrieval of ion production rate information, and in suitable circumstances, such as marine air or on balloon ascents, air conductivity measurements provide a measure of CR ion production. Routine air conductivity measurements were made by the UK Meteorological Office (Dobson 1914) from the first decade of the twentieth century using the Ebert (Ebert 1901; Harrison 2007) or Wilson (Wilson 1908; Harrison and Ingram 2004) methods, and historical measurements from other occasional campaigns (Wilson 1908; Carse and MacOwan 1910; Ansel 1912; Wright and Smith 1916; Ault and Mauchly 1926) are also available.

2.1.2 Air Conductivity Measurements on Manned Balloon Ascents

Manned hydrogen-filled balloons provided the primary measurement platform for early research into the electrical properties of the atmosphere, including air conductivity (Harrison and Bennett 2007). The altitude reached was limited to about 10 km, as no oxygen was carried for the aeronauts. The first measurements of ion concentration were obtained using an Ebert ion counter (Ebert 1901), but a new air conductivity instrument was developed for balloon ascents by Gerdien (Gerdien 1905), which bears his name. The Gerdien condenser operates using an aspirated concentric cylinder electrode system, with an inner, well-insulated electrode charged to a large potential from a battery. From the voltage decay time, the air conductivity was calculated (Chalmers 1967). Alternate measurements of the positive and negative conductivity were made by varying the polarity chose for the central electrodes' bias voltage. Modern balloon measurements of the ion concentration in the atmosphere (Rosen and Hofmann 1988; Ermakov et al. 1997) have yielded a great diversity of results. Even accounting for different latitudes and solar activity levels, the ion concentrations obtained are not consistent with each other, which appears likely to be due to the varying extent of aerosol pollution.

2.1.3 Measurement of Air Conductivity at Various Latitudes

Oceanic measurements of air conductivity using Gerdien instruments were made by geomagnetic survey ships from about 1907, notably on the voyages of the *Galilee* and *Carnegie*. Analysis of these air conductivity measurements showed an aerosol effect in the North Atlantic (Wait 1946), but this was not present in measurements made in the Pacific (Cobb and Wells 1970). Using equation (2), and assuming a mean ion mobility μ of 1.2 $cm^2\ V^{-1}\ s^{-1}$, q is found to be $1.6 \pm 0.2\ cm^{-3}\ s^{-1}$, which is close to the typical "modern" value for cosmic ray ion production at the ocean surface of 2 $cm^{-3}\ s^{-1}$ (Hensen and van der Hage 1994).

2.2 Direct Observations of the Ion Production Rate and Ionising Particle Fluxes in the Atmosphere

2.2.1 Early Investigations in the Atmosphere

Early quantitative investigations of CRs measured the ions produced in a fixed volume of gas, within a device known as an ionisation chamber. Victor Hess, who discovered CRs, used ionisation chambers on his balloon ascents, notably the landmark flight of 7th August 1912 (Hess 1912), from which the extra-terrestrial and non-solar origin of cosmic rays was confirmed.

An ionisation chamber contained a fixed amount of gas at atmospheric pressure, with a collecting electrode biased to a constant initial potential. The electrode's potential was measured using an electrometer. Radiation passing through the chamber generated ion pairs, some of which (unipolar ions of opposite sign to the collecting electrode potential) were collected by the electrode. The measured current was proportional to the number of ion pairs created (Smith 1966). Practical disadvantages of ionisation chambers were that they excluded the ionisation effect of the lower part of the CR energy spectrum (Simpson 2000), and radioactivity within the material comprising the chamber walls could lead to erroneous findings.

The ascent made by Hess on 7 August 1912 is an important event in the history of cosmic ray research. Three different ionisation chamber instruments were used to measure ionisation rate, and the ionisation was by γ-radiation due to the thick zinc walls of the ionisation chambers. One instrument was not made airtight and had thinner walls to allow "soft rays" (β-radiation) to penetrate. The ionisation rate profile, produced from the mean of the three instruments recordings averaged from 88 observations, is shown in Fig. 1.

Starting in the 1930s, investigations of CRs in the atmosphere were actively developed using ionisation chambers, Geiger counters, emulsions and other techniques. Unlike ionisation chambers measuring the rate of ion production, gas-discharged Geiger counters and scintillation counters return the flux of ionising particles. In 1933–1934, E. Regener found

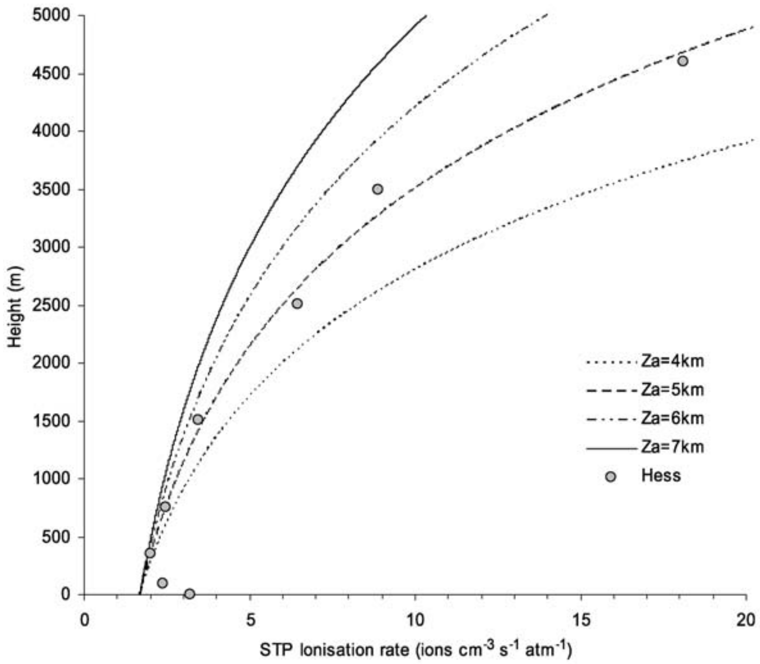

Fig. 1 Profile of the average volumetric ion production rate observations from the 7th August 1912 ascent by Victor Hess, compared with different modelled scale height reference altitudes Z_a (from Harrison and Bennett 2007)

a general form of altitude profile of ionising particle flux in the atmosphere (Regener 1934). However it was not until 1935 that Regener's pupil G. Pfotzer established for certain that the ionising particle flux in the atmosphere reached a maximum value at heights of $\sim$15 km (Pfotzer 1936). The dependence of particle flux or ionisation rate on the residual atmospheric depth[1] (or the height in the atmosphere) is called a transition curve with the Pfotzer maximum. Later cosmic ray observations in the atmosphere were directed to investigating the nature of the primary radiation, exploration of geomagnetic effects and the influence of solar activity on charged particle fluxes (Neher and Pickering 1942; Winckler and Anderson 1957; Nerukar and Webber 1964; Neher 1967; Neher 1971). In the spacecraft era these investigations became possible outside the Earth's atmosphere.

2.2.2 Ground-Based Cosmic Ray Flux Monitoring

As well as on the primary instrument in balloon ascents, ionisation chambers were also carried on geophysical exploration cruises. Chambers were carried on the geophysical and atmospheric electrical research ship *Carnegie*, on its voyages between 1915 and 1929. The ionisation chamber used on the *Carnegie* was a copper chamber of about 22 litres in volume, larger than those commonly used at the time (Ault and Mauchly 1926). "Penetrating radia-

[1] Atmospheric depth is the amount of the atmospheric matter in g/cm^2 overburden at a given level in the atmosphere. It is directly related to the barometric pressure so that the sea level (1013 hPa barometric pressure) corresponds to the atmospheric depth of 1033 g/cm^2.

tion" measurements were made on Carnegie cruises IV and VI, between 1915 and 1921 and show a variation with geomagnetic latitude, up to about $\sim 50°$ (Aplin et al. 2005).

In the middle of the 1930s a special ionisation chamber was developed for permanent ground-based monitoring of CR fluxes (Compton et al. 1934). Continuous data have been obtained from the identical chambers situated at Godhavn (Greenland), Cheltenham (Maryland), Huancayo (Peru), and Chistchurch (New Zealand). Their main drawback was a possible uncontrolled instrumental drift due to the "decay of radioactive contamination in the main chamber or in the balance chamber" (Forbush 1954; McCracken and Beer 2007), which is difficult to account for. Recovery of historical data to extend data series backwards in time is not a trivial task and yields controversial results. For example, Ahluwalia (1997) suggested, using data from ionisation chambers operating at Cheltenham/Fredericksburg (1937–1972) and Yakutsk (1953–1994), that the ionisation and the CR flux remained at roughly the same level throughout the last century (see also Okhlopkov and Stozhkov 2005). Recently however, McCracken and Beer (2007) revised this conclusion, using calibration against the intermittent balloon-borne ionisation data available since 1933 (e.g., Bowen et al. 1934), and found a significant trend in CR induced ionisation between 1930's and 1950's. The question on the long-term trend in ionisation data still remains open, and therefore recovering indirect sources of data is important in establishing the long-term behaviour of atmospheric ionisation (Harrison and Bennett 2007).

In the 1950s, J. Simpson established a world-wide ground-based neutron monitor network for permanent observation of cosmic ray temporal variations (Simpson 2000). This proved to be extremely fruitful both for cosmic ray investigation and study of links between cosmic rays and other solar and terrestrial phenomena. The neutron monitor network is now an indispensable source of information for investigation of both space and atmospheric CR effects. However the neutron monitor is sensitive to the nucleon component of CRs which, although substantial in the stratosphere, contributes little in the particle fluxes in the troposphere.

2.3 Ionising Particle Fluxes at Various Latitudes and Heights in the Atmosphere

2.3.1 Long-Term Cosmic Ray Observations in the Atmosphere

A detailed series of atmospheric ion production rate observations was conducted in the late 1960s (Neher 1967; Neher 1971; Anderson 1973). The measurement was performed using balloon-carried ionisation chambers. The standard chambers had steel walls 0.6 mm thick and were filled with air at 740 mm Hg pressure. The chamber temperature of 24°C was regulated to within ± 10°C during a balloon flight, and the temperature sensitivity of the chamber was less than 0.02%/°C. A latitude survey with long-term observations covering 1954–1969 was accomplished. In 1969–1970 another series of cosmic ray atmosphere ionisation and charged particle fluxes measurements was conducted by Lowder et al. (1972). Balloon flights were made at geomagnetic latitudes of 42°N and 52–54°N. These flights used an ionisation chamber similar to the one, used by the Neher group, but the results appeared about 20% lower than the Neher data although the claimed accuracy was ~ 5%. This discrepancy remains unexplained. Later we use the Neher results on ionisation rate for intercalibration.

There is a close relation between the charged particle flux and the ion production rate in the atmosphere (Bazilevskaya et al. 2000; Ermakov et al. 2007; Stozhkov et al. 2007). The most long-lasting observations of charged particles fluxes in the atmosphere (actually the ionising component of cosmic rays) have been performed by the cosmic ray group of Lebedev Physical Institute (LPI) from 1957 to the present time (Charakhchyan 1964; Bazilevskaya and Svirzhevskaya 1998; Stozhkov et al. 2004, 2007a). The experiment is directed to investigations of CR modulation by solar activity. Meteorological balloon programmes using radiosondes carrying a double-Geiger counter detector system are summarised in Table 1.

The charged particle detector consists of two Geiger counters with 0.05 $\mathrm{g\,cm^{-2}}$ steel walls arranged as a vertical telescope, with a 7 mm (2 $\mathrm{g\,cm^{-2}}$) thick aluminium filter inserted between the counters. The operating sizes of the counters are: 9.8 cm length and 1.8 cm in diameter. A single counter records the omnidirectional flux of charged particles: electrons with energy $E_e \geq 0.2$ MeV, protons with $E_p \geq 5$ MeV, and muons $E_m \geq 1.5$ MeV. The counters are also sensitive to γ-rays but with efficiency lower than 1%, whereas the efficiency for charged particle recording is ∼100%. Simulation of secondary CR fluxes in the atmosphere showed a good agreement with the fluxes measured by an omnidirectional counter (Desorgher et al. 2005). A telescope records a vertical flux of charged particles within a solid angle of about 1 sr: electrons with $E_e \geq 5$ MeV, protons with $E_p \geq 30$ MeV, and muons $E_m \geq 15$ MeV (muons with $E_m \leq 100$ MeV are virtually absent in the atmosphere). The radiosonde sensor returns data both on the omnidirectional and vertical fluxes of charged particles in the atmosphere alongside with the residual air pressure (the atmospheric depth), which can be converted to altitude using the standard atmosphere. Homogeneity of the data is maintained through the use of standard detectors (which were unchanged during the whole period of measurement) and careful calibration. Only omnidirectional counter data are presented in this paper.

Measurement of the Neher group and the LPI group overlapped during 1957–1969 allowing rather detailed comparison of the two series. Figure 2 demonstrates the flux of ionising particles, J, and the ion production rate, q and Q, at several latitudes as observed in the minimum of solar activity in 1964–1965. Neher performed a latitude survey in 1965 (Neher 1967). For comparison the CR data are taken from observations at the stationary locations of CR balloon measurements for $R_c = 0.6$ GV and $R_c = 2.4$ GV exactly at the months of Neher's observation. It should be noticed that there was no latitude attenuation in the CR fluxes between $R_c = 0.0$ GV and $R_c = 0.6$ GV because of the "knee-effect" (see below). For the lower latitudes, the CR measurements for 1964 (Charakhchyan et al. 1976a) are compared in Fig. 2 with the ion production data obtained in 1965. However at those latitudes the changes between 1964 and 1965 could not be large. The similarity in altitude dependence of CR flux, J, (left panel of Fig. 2) and ion production rate in the chamber at the atmospheric pressure, Q, (central panel of Fig. 2) is noticeable at middle and low latitudes ($R_c \geq 2.4$ GV). The shapes of transition curves for the two groups of data at the polar latitudes ($R_c = 0.0$–0.6 GV) and heights above 20 km are different because of the presence of low-energy, highly-ionising particles (especially, nuclei). The right panel of Fig. 2 gives the ion production rate in free air (ambient atmosphere), q, as derived from the ion chamber measurements. The ion production in free air depends on the flux of ionising particles and the density of ambient air, therefore, the maximum of transition curves shifts to lower altitudes. The relation between q and J is presented in Fig. 3 for different phases of solar activity cycle at polar latitudes ($R_c = 0.0$–0.6 GV) and for different R_c in the solar activity minimum. The ratio q/J is strongly dependent on the height H in the atmosphere and can be approximated as

$$q/J = A \exp(-B \cdot H). \quad (4)$$

It is seen in Fig. 3 that q/J slightly decreases with increase of R_c and growth of solar activity that is due to changes in the ionising particle energy spectrum and composition.

Table 1 Locations and operating modes of the LPI balloon CR measurements

Site	Coordinates	R_c (GV)	Period of measurements	Launches per week
Murmansk region	68°57′N 33°03′E 67°33′N 33°20′E	 0.6	1957–2002 since 2002	6–7*
Dolgoprudny, Moscow region	55°56′N 37°31′E	2.35	since 1957	5–7*
Alma-Ata, Kazakhstan	43°15′N 76°55′E	6.7	1962–1991	6
Mirny, Antarctica	66°34′S 92°55′E	0.03	since 1963	7*
Simeiz, Crimea	44°N 34°E	5.9	1958–1961, 1964 (Mar–Jul), 1969–1970	3–5
St.-Petersburg (Leningrad)	60°00′N 30°42′E	1.7	1964–1970	3
Norilsk	69°N 88°E	0.6	1974–1982	3
Yerevan, Armenia	40°10′N 44°30′E	7.6	1976–1989	3
Tixie-Bay	71°36′N 128°54′E	0.5	1978–1987	3
Dalnerechensk	45°52′N 133°44′E	7.35	1978–1982	1–3
Barentzburg, Svalbard	78°36′N 16°24′E	0.06	1982 (May), 1983 (Mar–Jul)	2–3
Campinas, Brazil	23°00′S 47°08′W	10.9	1988–1989, 1990–1991	1–3 occasionally
Vostok, Antarctica	78°47S 106°87E	0	1980 (Jan–Feb)	7
Main latitude surveys		0.1–17	1962–1965, 1968–1969, 1970–1971, 1975–1976, 1979–1980, 1986–1987	

*From early 1990s, the launches were made 3–4 times weekly

Averaged over an 11-year cycle and over the latitude dependence, $A = 122.6 \pm 1.3$ cm^{-1}, $B = -0.152 \pm 0.001$ km^{-1}, H is in km, q in cm^{-3} s^{-1}, J in cm^{-2} s^{-1}. It should be stressed that expression (4) is not true for SEP events and electron precipitation. Using the approximation (4) and the results of ionising particle measurements, it is possible to derive the ion

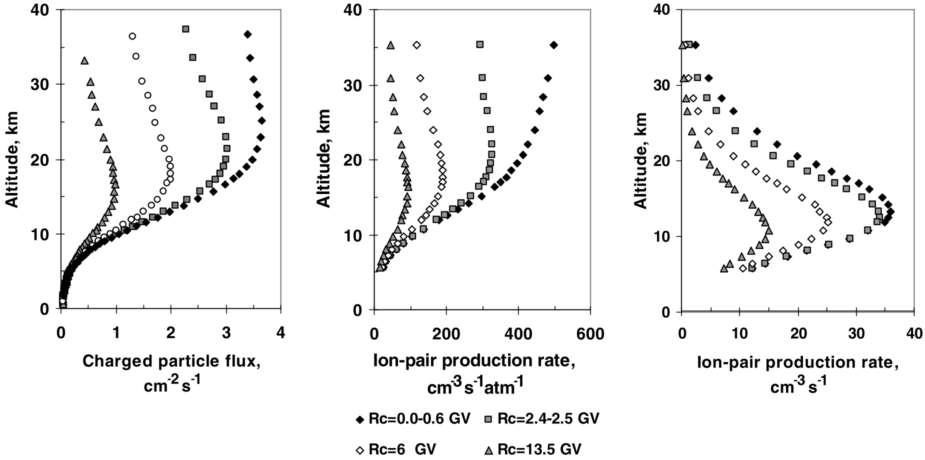

Fig. 2 *Left panel*: height dependence of ionising particle fluxes J at latitudes with different threshold cutoff rigidities R_c (LPI data). *Middle panel*: similar to the *left panel* but for the ion pair production rate in the ionisation chamber (Q) (Neher 1967, 1971). *Right panel*: the same as at the middle panel but converted to ionisation in free ambient air (q)

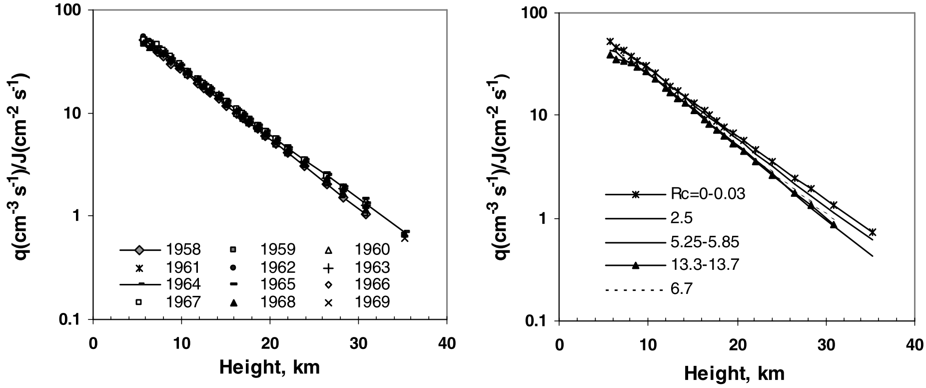

Fig. 3 Ratio of the ion production rate to the charged particle flux vs. altitude in the atmosphere. *Left panel*: results at polar latitudes during 1958–1969. *Right panel*: results for different latitudes in the solar activity minimum

production rate. An example is presented in Fig. 4 where the monthly averaged ion production rate inferred from the particles flux measurements is given for three heights in the atmosphere at polar latitude. The Neher data obtained during 1958–1969 are also plotted. Note that the ionisation rate q (cm^{-3}s^{-1}) at 24 km is smaller than at 6.5 and 11 km. This is because of the small density of ambient air at higher altitudes, and as can be seen in Fig. 2, this would not be so for the ionisation rate Q (cm^{-3} s^{-1} atm^{-1}) if the density effect were removed.

2.3.2 *Ionising Particles Fluxes at Various Latitudes in the Atmosphere*

A geomagnetic effect becomes apparent in the latitudinal dependence of particle fluxes which is different at higher and lower altitudes in the atmosphere. Results of observations

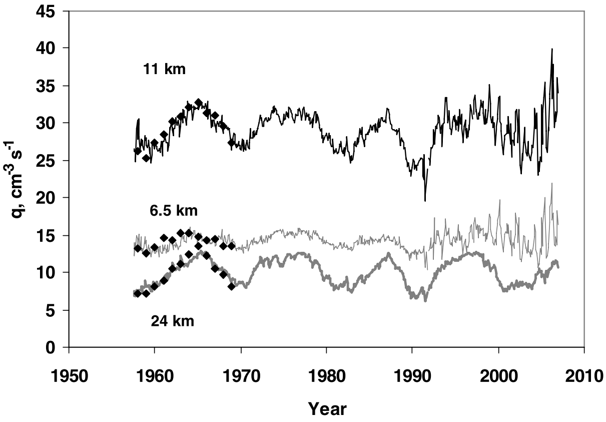

Fig. 4 Time dependence of ion production rate at 24, 11 and 6.5 km at polar latitude as inferred from observation of ionising particles fluxes (LPI monthly averaged data). Results of direct measurement of ionisation rate (Neher 1971) are plotted as *black diamonds*

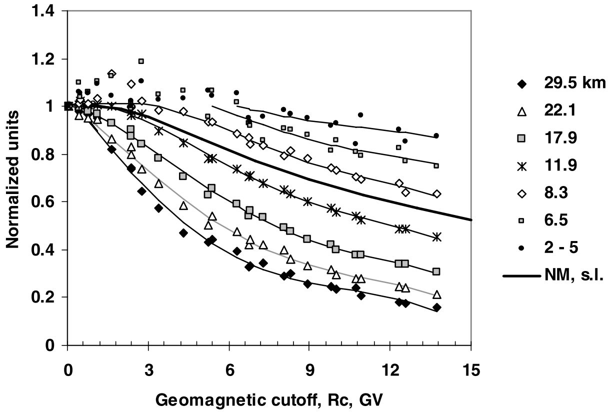

Fig. 5 Latitudinal attenuation (R_c dependence) in the CR ionising component at various heights in the atmosphere (*symbols* and *fitting lines*) in comparison with the effect in the neutron monitor count rates (*black solid curve*, Stoker 1994). Data are normalised at $R_c = 0$ GV

taken during the latitudinal survey in 1987 (Golenkov et al. 1990) normalised to values at $R_c = 0$ GV are plotted in Fig. 5. The balloons were launched from a ship, so the results are not affected by background radioactivity from the continental crust, but the sampling is still poor in the lower altitude. It is seen that the particle flux is virtually constant below a certain value of R_c. This is the CR knee-effect. At high altitudes, the knee-effect is due to the flat CR energy spectrum around hundreds of MeV (rigidity $\sim$1 GV). While proceeding to lower altitude, the knee shifts to higher R_c since the progenies of low energy primary particles cannot reach these altitudes. The latitude attenuation in the neutron monitor count rates also measured in the solar activity minimum is presented in Fig. 5 by the solid black curve (Stoker 1994).

2.4 Temporal Variations of Ionising Particle Fluxes in the Atmosphere

Figure 6 presents monthly averaged ionising particle fluxes at selected heights in the atmosphere over the Murmansk region (LPI results). Days when solar or magnetospheric particles invaded atmosphere are excluded. At the altitudes above $\sim$8 km, the most prominent variation is an 11-year solar cycle which is in opposite phase to the sunspot number. An important characteristic feature of the long-term solar modulation of CR fluxes—variation in shape between subsequent CR intensity maxima, is clearly evident in Fig. 6. In epochs

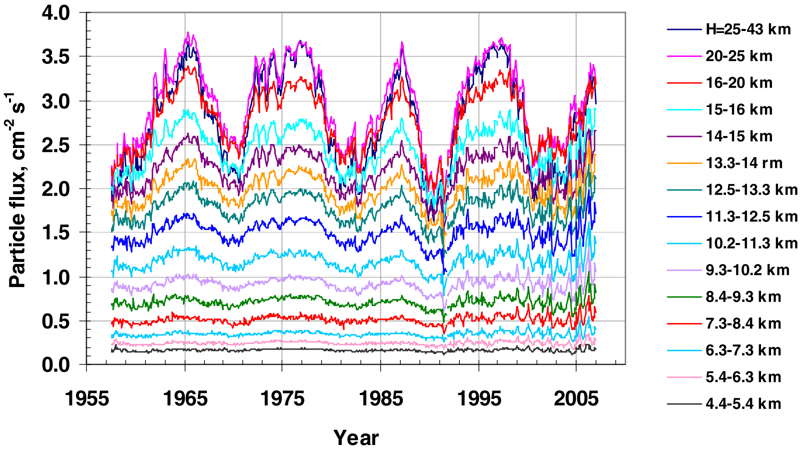

Fig. 6 Monthly averaged fluxes of ionising particles in the atmosphere over Murmansk region as measured by an omnidirectional Geiger counter. *Various colors* present fluxes at various heights. Days when solar or magnetospheric particles invaded atmosphere are excluded from averaging

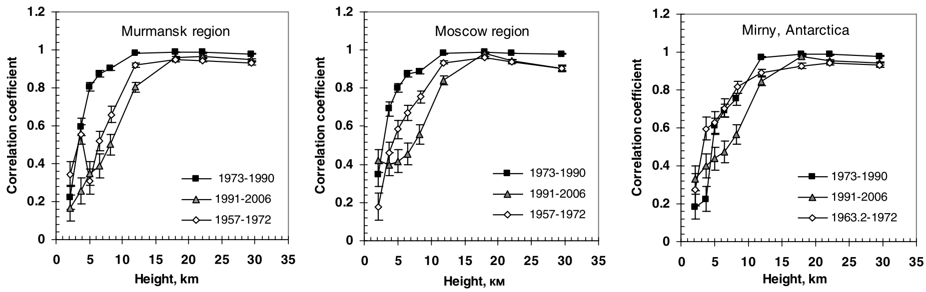

Fig. 7 Correlation between the monthly means of ground-based polar neutron monitor data and fluxes of ionising particles at various heights in the atmosphere. (After Bazilevskaya et al. 2007)

with a positive magnetic field in the northern hemisphere of the Sun (the 1970s and 1990s) the 11-year maximum in CR intensity has a flat top, whereas during the alternate epochs the maximum has a sharp peak (e.g., in 1965, 1987, and forthcoming one in 2007 or later). A similar behaviour should be expected in any atmospheric phenomenon closely connected to CRs.

At altitudes below ∼6 km, the 11-year modulation becomes weak. Its amplitude is about 15% and it is masked by some other variations. As demonstrated in Fig. 7 above 15 km the correlation coefficient between the values of charged particle flux in the stratosphere and count rates of a ground-based neutron monitor is close to 1 for both high- and mid-latitude stations. While moving deeper in the atmosphere the correlation decreases. Moreover, the height dependence of the correlation coefficient was different before 1973, in 1973–1991, and after 1991. Therefore, neutron monitor data may be correctly used as a proxy of ionising component only for the stratospheric altitudes. No significant trend is observed in the charged particle fluxes in the atmosphere during the last 50 years.

The most prominent short-term changes of the CR flux are Forbush decreases caused by disturbances in the interplanetary magnetic field. Forbush decreases modulate CR with

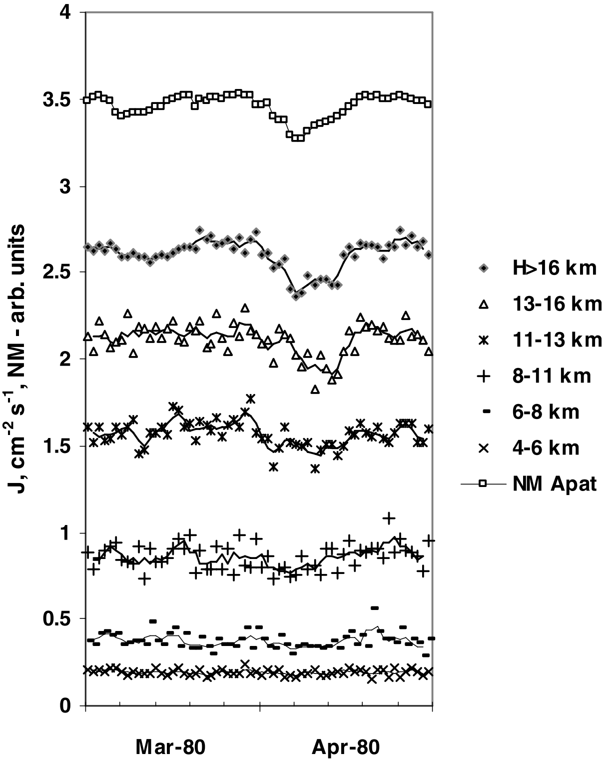

Fig. 8 Daily data of the Apatity neutron monitor (*upper curve*, arbitrary units) and charged particle fluxes at various atmospheric heights. *Symbols* are the daily data, averaged for Murmansk region and obs. Mirny (Antarctica). *Curves* are the 3-day running mean

rather high energy thus affecting the atmospheric particle flux at all altitudes and latitudes. The amplitude of a Forbush decrease is only weakly attenuated in the atmosphere. Figure 8 presents a Forbush decrease as recorded by the sea-level Apatity neutron monitor (∼8%) along with simultaneous measurements by the LPI instrument at several heights in the atmosphere. The amplitude of the Forbush decrease is ∼13% at the heights above ∼16 km, and ∼11% at 6–8 km. However, the Forbush effect is hardly discernible in the LPI data at heights below 6 km because of presence of other variations and poor statistical accuracy.

Solar energetic particles (SEPs) intrude into the atmosphere sporadically (Bazilevskaya 2005). Most of SEPs are just absorbed in the atmosphere leading to the enhanced ionisation in the polar stratosphere. An example is given in Fig. 9. During the first hours after the solar flare start on 20 January 2005, the enhanced ionisation was observed over Murmansk region at the heights above 10 km, where protons with energy $E > 780$ MeV can penetrate. Next morning, 26 hours after the flare, ionisation was increased only above ∼23 km, where only protons with $E > 220$ MeV can arrive. Because of geomagnetic cutoff, only high-energy SEPs can reach the mid- and low-latitudes, and the SEP effect there is rare and short lasting. The SEP events happen more often in periods of high solar activity. Usually there are between 20 and 30 events for an 11-year solar cycle which produce additional ionisation at heights below 30 km in the polar atmosphere. It should be noted, that only about half of them are powerful enough to essentially enhance the nucleonic component of the atmospheric cascade at the surface, leading to a ground level enhancement (GLE) of neutron monitor count rates.

Another kind of particle invasion in the atmosphere is precipitation of magnetospheric electrons (Makhmutov et al. 2001). Precipitating relativistic electrons form a maximum in

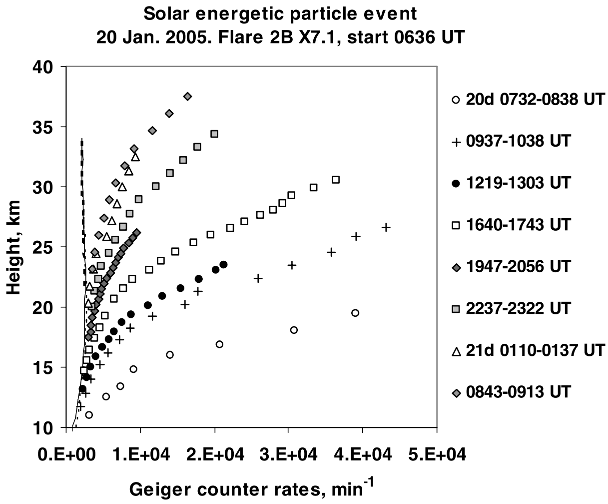

Fig. 9 Intrusion of solar energetic particles during the 20-Jan-2005 event into the atmosphere as recorded in Murmansk region by a Geiger counter versus heights. The *dashed curve* presents a background due to galactic cosmic rays. *Symbols* refer to different time of observations

the ion production rate at heights between 50 and 90 km where their energy deposit may sometimes be higher than that of solar UV radiation and CRII. The second maximum in the ion production at about 30 km is due to the bremsstrahlung X-rays generated by precipitating electrons. Here the ionisation rate from X-rays is significantly less than that from galactic CRs (Pesnell et al. 2001). Gamma and X-rays are also generated by galactic CRs in the cascades in the atmosphere, the photon fluxes ($E > 20$ keV) being an order of magnitude higher than the electron ($E > 200$ keV) fluxes (Charakhchyan et al. 1976b). Roughly speaking, the electron and photon fluxes are in equilibrium in the atmosphere. While interacting with the air atoms, X-ray photons generate Compton and photo-electrons; γ-ray photons with $E > 1$ MeV can produce an electron-positron pair. Most of these charged particles have energy below the thresholds of the LPI measurements.

As it is seen in Fig. 6 charged particle fluxes in the atmosphere became more disturbed after 1990, especially at the heights below ~12 km. In the same period, the balloon launches became less frequent (see Table 1) therefore enhanced variability could be due to less observational accuracy. However, the disturbances appear to be very similar at Murmansk and Moscow regions and, besides, an annual periodicity can be traced, especially beginning from 1998. There is no such periodicity at Mirny (Antarctica) although an enhanced level of variability is also present. This can be clearly seen in Fig. 10 where the time history of ionising fluxes in the troposphere of Murmansk and Moscow regions (upper panel) and of Mirny (lower panel) is presented. It should be noted that the annual oscillation at the heights 2–6 km is much lower in the Antarctic (~3%) than in the Arctic (8–9%) (Fleming et al. 1990). Maximum particle fluxes are observed in the winter period in the northern hemisphere as it is expected due to the temperature effect of cosmic ray muon component. However, the expected effect is ~5% which is consistent with observations in 1973–1991 (Kurguzova and Charakhchyan 1983). In 1999–2002 and 2005–2006 the annual change in the ionising particle fluxes comprised 15–10%, and ~30%, respectively. This annual temperature oscillation can be traced in the atmosphere up to 10–15 km. At the moment, the nature of these variations is not clear.

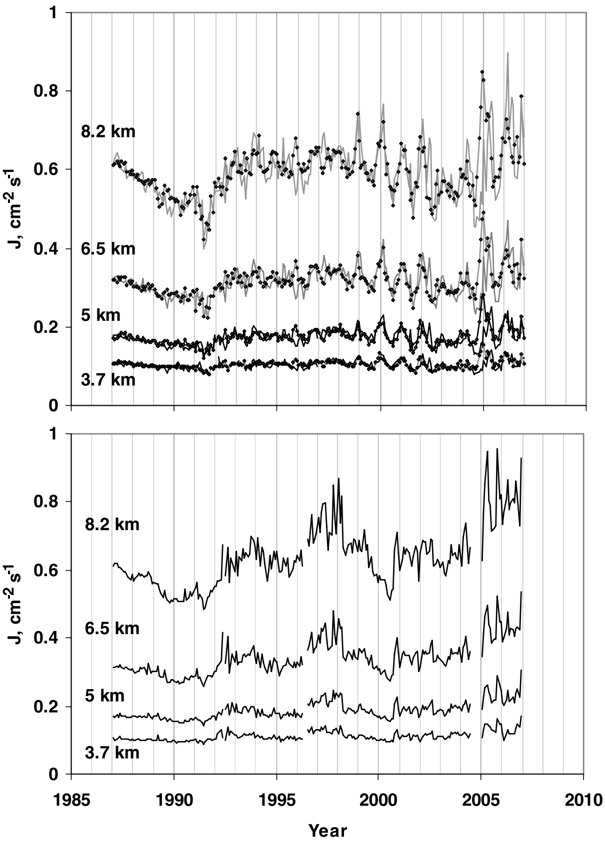

Fig. 10 Temporal variations of ionising particle fluxes in the troposphere in 1987–2006. *Upper panel*: Murmansk region (*solid curve*) and Moscow region (*curve with rhombs*); *lower panel*: Mirny (Antarctica)

3 Modelling of Cosmic Ray Induced Ionisation

3.1 Atmospheric Cascade Induced by Cosmic Rays

When an energetic CR particle enters the atmosphere, it first moves straight in the upper layers suffering mostly ionisation energy losses that lead to ionisation of the ambient rarefied air. Therefore, the cosmic ray induced ionisation (CRII) of the upper atmospheric layers (above approximately 25 km) can be easily calculated analytically (Velinov and Mateev 1990). However, after traversing some amount of matter (the nuclear interaction mean free path is of the order of 100 g/cm^2 for a proton in the air) the CR particle may collide with a nucleus in the atmosphere, producing a number of secondaries. These secondaries have their own fate in the atmosphere, in particular they may suffer further collisions and interactions forming the so-called atmospheric cascade (Dorman 2004). Because of the large amount of matter in the Earth's atmosphere (1033 g/cm^2) the number of subsequent interactions can be large leading to a fully developed cascade consisting of secondary rather than primary particles. It is common to divide the cascade into three main components: the "soft" or electromagnetic component which consists of electrons, positrons and photons; the "hard" or muon component consisting of muons (pions are short-lived and decay almost immediately); and the "hadronic" nucleonic component consisting mostly of superthermal protons and neutrons. All charged secondaries ionise the ambient air and their relative role changes with the

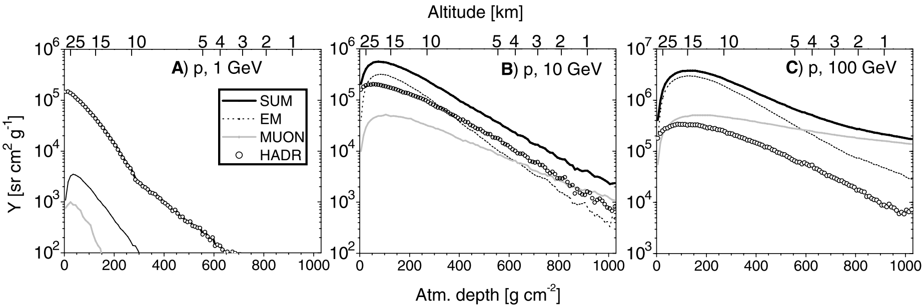

Fig. 11 Ionisation by atmospheric cascade induced by primary CR protons with energy 1 GeV, 10 GeV and 100 GeV (resp. *left to right panels*) isotropically impinging on the Earth's atmosphere (computations by Usoskin and Kovaltsov 2006). *Curves* represent: ionisation by the electromagnetic (*dotted*), the muon (*grey*) and the hadronic components (*open dots*) of the cascade, as well as the total ionisation (*solid curve*). *Top X-axis* depicts approximate altitude for the standard static atmosphere

energy of primary particles and altitude in the atmosphere. When describing the cascade it is usual to deal with the residual atmospheric depth rather than with the altitude. The reason is that the development of cascade is mostly defined by the amount of matter traversed, while the actual altitude may vary depending on the exact atmospheric density profile. Figure 11, based on a full Monte-Carlo simulation of the atmospheric cascade (Usoskin and Kovaltsov, 2006—see next section) shows the relative role of the three components in ionising the air as a function of the atmospheric depth for three energies of the primary CR proton. For low-energy cosmic rays, CRII is defined only by the hadronic component (Fig. 11A) at all altitudes. The role of the other components increases with increasing CR energy. All the three components are equally important at middle energies of CR particles (Fig. 11B), but they dominate at different altitudes: the soft component at high altitudes ($h < 300$ g/cm^2), the muon component near the sea level ($h > 900$ g/cm^2), and the hadronic component in the troposphere. The ionisation induced by high-energy cosmic rays (Fig. 11C) is dominated by secondary muons in the lower troposphere ($h > 600$ g/cm^2) and by the electromagnetic component at higher altitudes, while the contribution from the hadronic component can be neglected in this case. Therefore, all the three components are important, but play their roles at different altitudes and different energy ranges of primary particles.

3.2 Numerical Models

Because of the atmospheric cascade it is a complicated task to model the CRII process. Earlier it was common to use an analytical approximation for the cascade (O'Brien 1979, 2005), but such models become less reliable in the lower atmosphere. With the progress in computational methods and knowledge of nuclear processes, precise models, based on full Monte-Carlo simulations of the atmospheric cascade, have been developed. There are currently two basic numerical approaches to CRII Monte-Carlo simulations. One is the Bern model (Desorgher et al. 2005) called ATMOCOSMIC/ PLANETOCOSMIC, which is based on the GEANT-4 simulation package. The PLANETOCOSMIC code is available at http://cosray.unibe.ch/~laurent/planetocosmics/. Another approach is based on the CORSIKA+FLUKA Monte-Carlo package and has been primarily developed as the Oulu model (Usoskin et al. 2004a; Usoskin and Kovaltsov 2006) and later adopted by other groups (Mishev and Velinov 2007). The two models have recently been the subject of a comparison (Usoskin et al. 2008b) in the framework of the COST-724 action (see http://www.cost.esf.org). Results of the two simulations agree within 10%, the difference being mainly due to the different atmospheric models used and, to a lesser extent, to different cross-section approximations in CORSIKA and GEANT-4 packages. Note that an analytical approximation model of CRII (O'Brien 2005) also shows a reasonable agreement with the present models, especially at higher altitudes.

Generally CRII rate (number of ion pairs produced in one gram of the ambient air per second) at a given atmospheric depth h can be represented in as follows:

$$q(h, \phi, R_c) = \sum_i \int_{E_{c,i}}^{\infty} S_i(E, \phi) Y_i(h, E)\, dE, \tag{5}$$

where the summation is performed over different i-th species of CR (protons, α-particles, heavier species), $Y_i(h, E)$ is the ionisation yield function (the number of ion pairs produced at altitude h in the atmosphere by one primary CR particle of the i-th type, isotropically impinging on the Earth's magnetosphere with kinetic energy E), $S_i(E, \phi)$ is the differential energy spectrum[2] of galactic cosmic rays in the Earth's vicinity (given in units of [cm^2 sec sr (GeV/nuc)]$^{-1}$). Integration is performed above $E_{c,i}$, which is the kinetic energy of a particle of i-th type, corresponding to the local geomagnetic cutoff rigidity R_c. Full details of the CRII computations, including a detailed numerical procedure and tabulated Y, are given in Usoskin and Kovaltsov (2006). Note that CRII at a given location and time depends on three variables: altitude (atmospheric depth h) via the integrand yield function Y, geographical location via the geomagnetic cutoff rigidity R_c (integration limits), and solar modulation (the modulation potential ϕ) via the integrand CR spectrum S. Since these three variables are mutually independent, they can be separated in order to solve the problem numerically in an efficient way.

Firstly, using a full Monte-Carlo simulation of the atmospheric cascade, one can compute the yield function Y depending on the atmospheric depth and energy of primary CR particles (see Fig. 11). Then the ionisation can be computed for any given time (i.e., CR modulation potential ϕ) and geographical location (i.e., geomagnetic cutoff rigidity R_c) by integrating equation (5). The effective energy of primary cosmic rays available for ionisation varies with the atmospheric depth, being about 1 GeV/nuc for stratosphere and increasing to about 10–30 GeV/nuc in the low troposphere. An example[3] of the dependence of CRII on ϕ and R_c is shown in Fig. 12 for two atmospheric depths of 300 and 700 g/cm^2. One can see that CRII may vary by a factor of two between polar region at solar minimum and equatorial region during solar maximum. On the other hand, CRII is very sensitive to the altitude as apparent from Fig. 13. The ionisation rate varies by two orders of magnitude between sea level and the maximum (known as the Pfotzer maximum) which is located at 18–20 km in polar regions and moves slightly downwards (about 15 km) in equatorial regions.

3.3 Comparison with Measurements

The modeled CRII can be compared with real measurements of the ionisation rate in the atmosphere. Figure 14 shows a comparison of the model calculations (curves) to the measurements (symbols) for three different conditions: in the polar atmosphere during a solar maximum (panel A); in the equatorial atmosphere during a solar minimum (panel B); and

[2]The CR spectrum can be uniquely parameterised via the modulation potential ϕ, which is ultimately defined by the solar magnetic activity—see Usoskin et al. (2005). Note that ϕ grows with the solar magnetic activity.

[3]Results in Figs. 12–16 is given for the Oulu model but the Bern model yields essentially similar results.

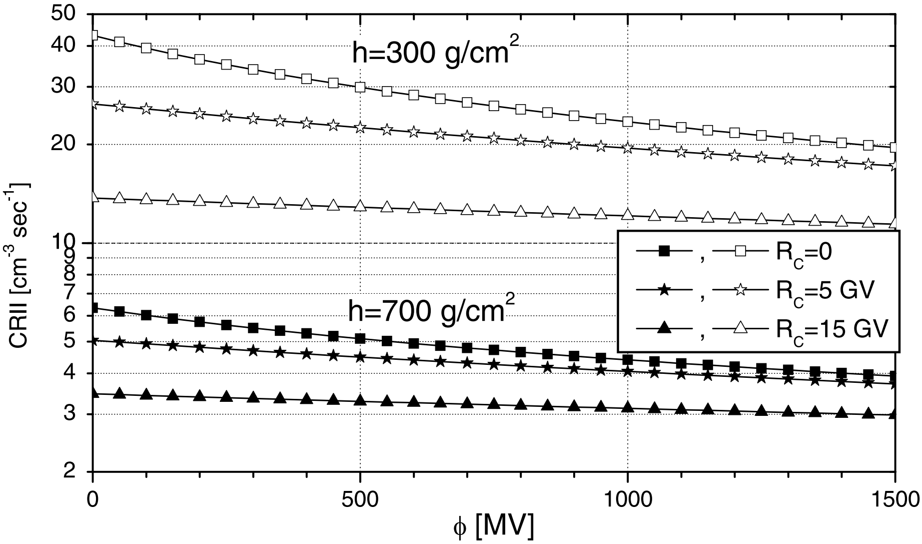

Fig. 12 Modelled CRII as a function of the modulation potential ϕ for different locations and altitudes (computations by Usoskin and Kovaltsov 2006) for two values of the atmospheric depth (700 g/cm^2—about 3 km altitude; and 300 g/cm^2—about 9 km). The results are shown for the geomagnetic pole ($R_c = 0$), mid-latitude ($R_c = 5$ GV, about 40° geomagnetic latitude) and equator ($R_c = 15$ GV)

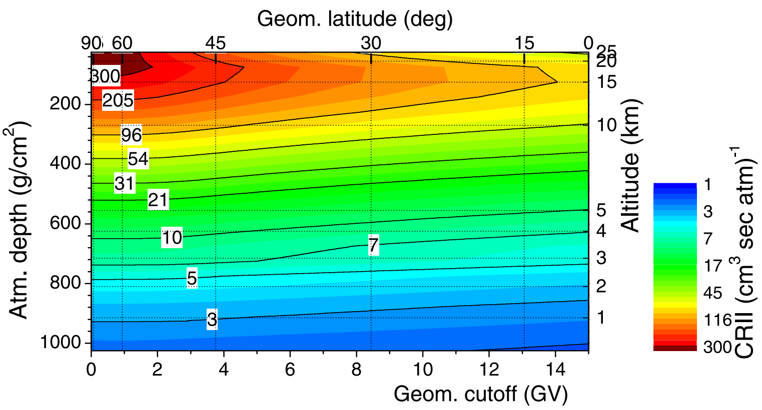

Fig. 13 Modelled CRII as a function of the atmospheric depth h (or altitude—*right axis*) and R_c (or geomagnetic latitude—*upper axis*) for medium CR modulation ($\phi = 500$ MV)

in the southern UK during moderate solar activity. One can see a good agreement between the model and the measured ionisation rates below $h = 50$ g/cm^2 (about 20 km) for all conditions. We note that individual measurements, performed during short balloon flights, can vary depending, e.g., on the exact atmospheric profile, the instrumentation used, exact energy spectrum of CR, etc. On the other hand, the model CRII is computed for average conditions (the standard atmospheric profile, mean modulation potential). Therefore, the observed agreement within 10% is considered good. This is clearly seen in Fig. 14c where the ionisation measured during a single balloon flight is shown and depicts some layer-like

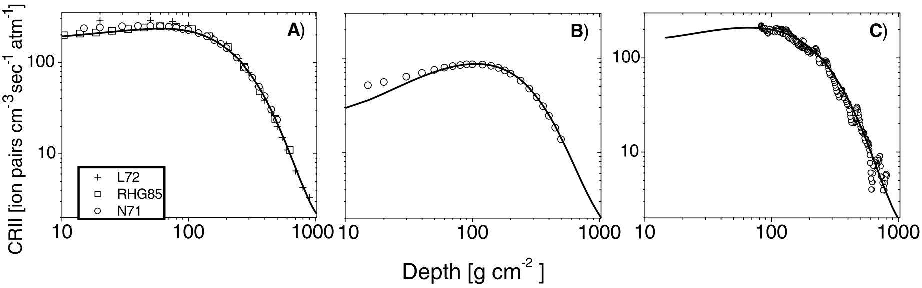

Fig. 14 Agreement between measured (*symbols*) and modeled (*curves*) CRII for different conditions. **A)** Polar region at solar maximum. *Symbols* denote measurements by (L72—Lowder et al. 1972), (RHG85—Rosen et al. 1985), (N71—Neher, 1971), *curve* depicts CRII at $R_c = 1$ GV, $\phi = 1000$ MV. **B**) Equatorial region at solar minimum. *Dots* denote measurements by Neher (1971) in July 1965. Curve depicts CRII at $R_c = 15$ GV, $\phi = 420$ MV. **C**) Medium conditions. Dots denote measurements at the University of Reading (Harrison 2005) in the afternoon 18/08/2005. Curve depicts CRII at $R_c = 2.5$ GV and $\phi = 650$ MV

structures and strong fluctuations, especially in the low troposphere. However, the measurements lie close to the modeled smooth curve. In order to precisely reproduce an individual observation, one needs to know the exact atmospheric density and temperature profile appropriate to the instantaneous measurement. In the upper part of the atmosphere (above 50 g/cm^2), the model yields somewhat lower CRII than the measurements. This is most likely related to the action of additional ionising agents other than CR (e.g., solar UV-radiation, precipitating low-energetic particles), and possibly due to a wall effect of the detector. Thus, the model CRII calculations agree (within 10%) with the actual measurements in the whole range of possible parameters, for the troposphere and lower stratosphere, and slightly underestimate the ionisation at altitudes above 50 g/cm^2 (20 km), where other ionising agents become important.

The fact that the model results agree with the real measurements in the wide range of parameters as well as between the different models confirms the validity of the models and their applicability in studying ionisation effects due to cosmic rays in the atmosphere.

3.4 Long-Term Changes

CRII varies quite essentially both spatially (altitude and geomagnetic latitude) and temporally. The temporal variations are dominated by the 11-year solar cycle as discussed in Sect. 2, but CRII demonstrates changes also on longer time scales. E.g., a significant long-term decreasing trend was reported in the ionisation data between 1933 and 1950's (McCracken and Beer 2007). Using intermittent balloon measurements of the air conductivity, Harrison and Bennett (2007) found a systematic decrease of ionisation by roughly 0.15%/year between 1910 and 1950 associated with increasing solar activity. However, because of the lack of systematic direct or indirect measurements, it is difficult to study longer term changes using real data. On the other hand, CRII can be realistically modelled in the past using independent estimates of solar activity and geomagnetic field variations. An example of the modelled CRII variations on multi-centennial time scale is shown in Fig. 15, that is consistent with the observed trends in the first half of 20-th century. One can see that the long-term variations of CRII are comparable or even exceed the 11-year cycle range. The estimated CRII during the Maunder minimum of solar activity (1645–1715) was nearly constant at the level of ≈24% greater than during the recent minima or 31% higher than the average ionisation rate for the last 50 years. It is noteworthy that the period after 1700 AD

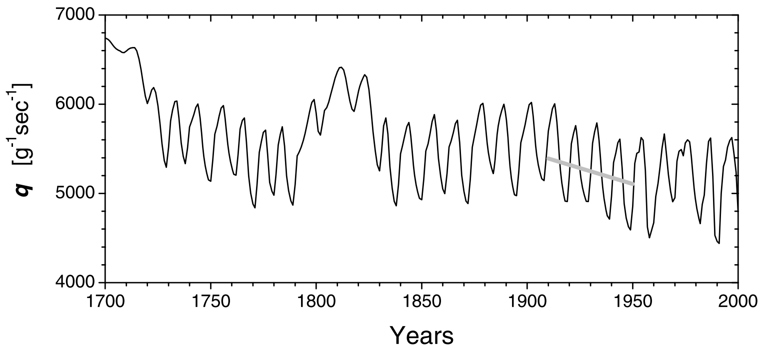

Fig. 15 Time profile of CRII in polar region at $h = 700$ g/cm^2 since 1700 AD computed using the solar modulation reconstruction by Usoskin et al. (2002) (adapted from Usoskin and Kovaltsov 2006). *Grey line* illustrates the 0.15%/year decrease of the atmospheric ionisation between 1910 and 1950 (Harrison and Bennett 2007)

shown in Fig. 15 includes the whole range of solar activity variability, from the deep Maunder minimum to the modern Grand maximum of solar activity (Usoskin et al. 2007). Therefore, the CRII variability due to solar activity changes is not expected to exceed this range. However, changes of the geomagnetic field, leading to the changing cutoff rigidity R_c, can be also quite significant and even more important on the centennial-millennial time scale than solar variability, especially in mid-latitude regions (Kovaltsov and Usoskin 2007; Usoskin et al. 2008a). Because of these geomagnetic changes, the long-term variability of CRII may depend on the geographical location and its effects on, e.g., climate should be studied regionally as global averaging may smear out the effect.

Thus, CRII may undergo variations on long-term timescales caused by both solar activity and geomagnetic changes.

3.5 Effect of Solar Energetic Particles

While the ionisation due to galactic CR is always present in the atmosphere, strong transient changes of the fluxes of energetic particles can occur related to solar eruptive phenomenon (solar flares or coronal mass ejections). In particular SEP events can lead to significant increase of the atmosphere ionisation especially at high altitude in the polar atmosphere (Schröter et al. 2006). As an example, we consider here the ionisation effect of a severe SEP/GLE event of 20/01/2005, which was one of the strongest GLEs ever observed. Time profile of the neutron monitor count rate for this event is shown in Fig. 16A. During the peak at 06:55–07:00 UT, the flux of cosmic ray as measured by the South Pole NM increased by about 500% due to arrival of highly anisotropic SEPs (Vashenyuk et al. 2006; Plainaki et al. 2007). The gradual decay of the GLE event over a few hours was due to nearly isotropic component of SEP. A noteworthy aspect is that the GLE occurred during the continuing effect of a strong Forbush decrease caused by the interplanetary shock, when the CR level was reduced by 10–15% for a week (Fig. 16A). The net effect of the sequence of events is negative in the neutron monitor count rate (i.e., the long-lasting Forbush decrease over-compensates the CR increase during the transient GLE). Figure 16B shows the calculated net CRII effect of the active period of 18–23 Jan. 2005 with respect to the undisturbed period 12–17 Jan. (the ratio between the former and the latter is shown) for different atmospheric depths and geomagnetic latitudes. One can see that the event-integrated net effect is negative in the entire troposphere, even in the polar region. Strong positive effect of

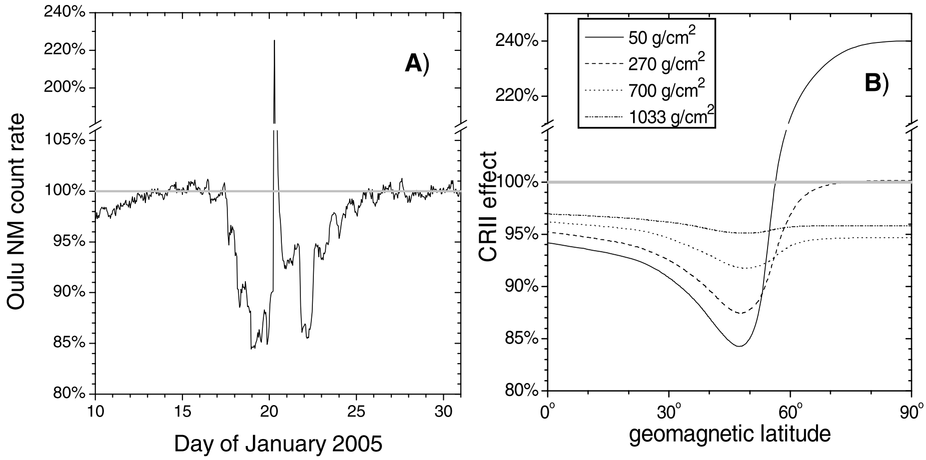

Fig. 16 Combined effect of solar and galactic CR for the event of January 2005. **A**) Count rate of the Oulu NM in January 2005, normalised to the period 12–17 Jan. 2005. **B**) Ionisation effect (see text) as a function of the atmospheric depth (different *curves* as denoted in the legend) and geomagnetic latitude (X-axis). Note breaks in the Y-axis

enhanced CRII exists only in polar stratosphere where it may become very strong at high altitudes. Thus, the net event-integrated ionisation effect of SEP is relatively small or even negative.

On the other hand, many processes, including chemistry of the upper atmosphere, are sensitive not only to the time-integrated effect but also to the instantaneous flux of particles, which can be enhanced by orders of magnitude during the peak phase of event. The peak phase of GLE is often highly anisotropic so that a strong collimated beam of SEPs impinges on a relatively small spot in the atmosphere. The peak effects of such a beam are considered below for the same event of 20/01/2005. The spectrum and the angular distribution of solar protons outside the magnetosphere have been computed from the neutron monitor network data (Bütikofer et al. 2008). For the peak time the pitch angle distribution of the solar protons was very narrow with the flux at 55° pitch angle being only 10% of the flux in the main direction. Using the Bern CRII model, the ionisation rate was computed globally in a 5° × 5° geographic grid (Fig. 17) for the upper troposphere. The top panel represents the momentary ionisation rate accounting for both SEP and CR fluxes, while in the bottom panel the ionisation induced only by CR is plotted as reference. One can see that the increase in CRII due to SEPs strongly depends on the location and, for this particular event, can be up to a factor of 100 in a very localised region around 70°S 140°E. This is a direct consequence of the high anisotropy of the solar particles at this specific time.

Thus, the ionisation effect of SEP events is local and of most importance in the polar atmosphere. The global effect of CRII solar particles is tiny, even for the most severe events.

3.6 Application to Other Planets

Galactic cosmic rays play also a major role in the ionisation of the atmosphere of other planets and moons of our solar system (Aplin 2005). Several authors have modeled this ionisation in the past. Capone et al. (1977, 1979) have computed the contribution of cosmic rays to the ionisation of the atmosphere of giant planets. The cosmic ray induced ionisation of the atmosphere of Venus and Titan has been calculated by Borucki et al. (1982, 1987) by

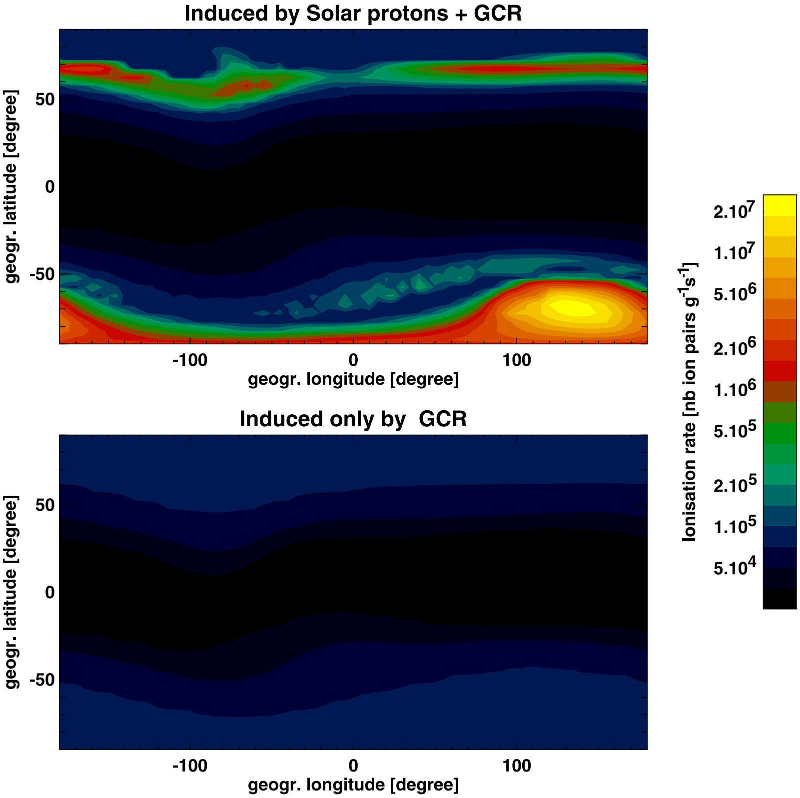

Fig. 17 Computed ionisation rate of the upper troposphere ($h = 300$ g/cm^2), at 06:55 UT on January 20, 2005: the total ionisation rate (*top panel*) and that due to GCR only (*bottom panel*)

using a modified version of the code developed for the Earth's atmosphere by O'Brien et al. (1979). The same Earth code has been modified by Molina-Cuberos et al. (1999, 2001) to compute the ionisation of the Titan's and Martian atmosphere.

When computing the ionisation of the atmosphere by cosmic rays for other planetary bodies, some important differences have to be taken into account compared to the Earth. The first difference is that the amplitude of the modulation of the cosmic rays by the heliosphere is decreasing with the solar distance, resulting in a higher flux of cosmic rays in the outer heliosphere. While the flux of GCR is roughly similar at Earth's and Mars's orbits, it is not true for other planets since the GCR intensity increases with the heliocentric distance. Another important difference is the presence or not of a planetary dynamo. Mars does not have an internal magnetic field any more, and even the high crustal field on some region of Mars is not high enough to deflect significantly cosmic rays (Acuňa et al. 2001; Dartnell et al. 2007). In the case of Jupiter the internal magnetic field is much higher than the geomagnetic field leading to a maximum cut-off rigidity (at the equator) of the order of 1 TV (roughly two order of magnitude higher than on Earth). To compute the access of CR to the moon of a magnetised planet, the positions of the moon's orbit in the magnetosphere of the planet has also to be known. On Titan the magnetic shielding effect can be neglected, as only a part of its orbits is contained within the Saturnian magnetosphere, in a region where the field is too low to significantly deflect cosmic rays (Backes et al. 2005). Finally the most obvious difference to consider is the variation of the composition and of the density profile of the atmosphere itself.

A cosmic ray code that can treat all the planets and would be available for all the scientific community does not exist yet. The PLANETOCOSMICS code, based on the Geant4 Monte Carlo toolkit, has been recently developed to provide such an application. It simulates the electromagnetic and hadronic interaction of energetic particles with the Earth, Mars and Mercury (Desorgher et al. 2005; Dartnell et al. 2007; Gurtner et al. 2005; Gurtner et al. 2006), and an extension to Jupiter, Saturn and their satellites is under development. The code computes the magnetic shielding of the planet magnetosphere in function of position, the energy deposited by cosmic ray shower particles in the atmosphere and the soil (and therefore can be used to compute the ionisation rate), as well as the flux of any kind of particles at given depth and altitude in the atmosphere and in the soil. The source code for PLANETOCOSMICS can be downloaded from the url http://cosray.unibe.ch/ laurent/ planetocosmics.

4 Summary and Conclusions

More than 100 years of research in ionising particle behavior in the atmosphere has yielded a huge amount of observational data and general understanding of the related processes which control evolution of particle composition and their spatial-temporal distribution. Recognition of the role CR-induced ionisation plays in atmospheric processes, including cloudiness and precipitation requires careful and detailed analysis of ionising particles relation with the condition in the atmosphere. In spite of many correlations found between the particle flux temporal changes and various weather phenomena, no well-established physical connections and mechanisms are yet able to explain the observations. Monitoring of cosmic ray fluxes both with balloon-borne devices and ground-based installations gives a rich source of information for research in this field.

Dedicated simultaneous measurements of ion-production rate, aerosol concentration and ion properties, particularly independent measurements of ion concentration and mobility, should be obtained in the atmosphere.

Essential progress has been achieved recently in developing models of cosmic ray induced ionisation in the atmosphere. Models based on full Monte-Carlo simulation of the nucleonic-electromagnetic-muon cascade induced by CR in the atmosphere are able to properly simulate the 3D time dependent ionisation rate with high accuracy in the troposphere and lower stratosphere (below $\sim$20 km). Thus, the modern CRII models provide a reliable tool to study ionisation effects due to cosmic rays in the atmosphere.

Modelling based on the neutron monitor data provides properties of the CR nucleon component. As shown in this paper, fluxes of the ionising CR component in the atmosphere demonstrate existence of both long-term and short-term variations which are not reflected by the neutron monitors. Further work is needed to understand nature of these variations and to input the proper parameters in the models.

Acknowledgements The LPI group is partly supported by the Russian Foundation for Basic Research (grants 08-02-00054, 08-02-00418, 08-02-91006, 08-02-10018, 07-02-01019) and the Program of Presidium RAS "Neutrino physics". Support from the Academy of Finland and the Finnish Academy of Science and Letters Vilho, Yrjö and Kalle Väisälä Foundation are gratefully acknowledged. GAK was partly supported by the Program of Presidium RAS N16-3-5.4. We are grateful to the teams operating ground based neutron monitors for their publicly available data used in this work. LD, RB and EOF acknowledge support by the Swiss National Foundation (grants 2000020-105435/1, 200020-113704/1), by the Swiss State Secretariat for Education and Research (grant COST-724/C05. 0034), and by the COST-724 action.

References

M.H. Acuña et al., J. Geophys. Res. **106**, 23403 (2001)
H.S. Ahluwalia, J. Geophys. Res. **102**, 24229 (1997)
H.R. Anderson, J. Geophys. Res. **78**, 3558 (1973)
A. Ansel, *Die luftelektrischen und meteorologischen Ergebnisse der Beobachtungen in Island vom 10. Mai bis 2. Juni 1910 anlaßlich des Durchganges des Halleyschen Kometen*, Nachrichten von der Gesellschaft der Wissenschaften zu Göttingen, Mathematisch-Physikalische Klasse 1912, 42 (1912)
K.L. Aplin, Surv. Geophys. **27**, 63 (2005)
K.L. Aplin, R.G. Harrison, A.J. Bennett, Adv. Space Res. **35**, 1484 (2005)
J.P. Ault, S.J. Mauchly, *Atmospheric-electric results obtained aboard the Carnegie 1915–1921*. Carnegie Institution of Washington publication **175**, 3 (1926)
H. Backes, F.M. Neubauer, M.K. Dougherty et al., Science **308**, 992 (2005)
G.A. Bazilevskaya, Adv. Space Res. **35**, 458 (2005)
G.A. Bazilevskaya, A.K. Svirzhevskaya, Space Sci. Rev. **85**, 431 (1998)
G.A. Bazilevskaya, M.B. Krainev, V.S. Makhmutov, J. Atmos. Sol.-Terr. Phys. **62**, 1577 (2000)
G.A. Bazilevskaya, M.B. Krainev, V.S. Makhmutov, A.K. Svirzhevskaya, N.S. Svirzhevsky, Y.I. Stozhkov, Variations of the charged particle fluxes in the Earth's troposphere. Bull. Lebedev Phys. Inst. **12**, 13 (2007)
W.J. Borucki, Z. Levin, R.C. Whitten, R.G. Keesee, L.A. Capone, O.B. Toon, J. Dubach, Icarus **51**, 302 (1982)
W.J. Borucki, Z. Levin, R.C. Whitten, R.G. Keesee, L.A. Capone, A.L. Summers, O.B. Toon, J. Dubach, Icarus **72**, 604 (1987)
I.S. Bowen, R. Millikan, H.V. Neher, Phys. Rev. **46**, 641 (1934)
R. Bütikofer, E.O. Flückiger, L. Desorgher, M.R. Moser, Sci. Total Environ. **391**, 177 (2008)
L.A. Capone, R.C. Whitten, S.S. Prasad, J. Dubach, Astrophys. J. **215**, 977 (1977)
L.A. Capone, J. Dubach, R.C. Whitten, S.S. Prasad, Icarus **39**, 433 (1979)
G.A. Carse, D. MacOwan, Proc. R. Soc. Edinb. **30**, 32, 460 (1910)
J.A. Chalmers, *Atmospheric Electricity* (Pergamon, Oxford, 1967)
A.N. Charakhchyan, Sov. Phys. Uspekhi **7**, 358 (1964)
A.N. Charakhchyan, G.A. Bazilevskaya, Y.I. Stozhkov, T.N. Charakhchyan, Trudy FIAN, Nauka, Moscow **88**, 3 (1976a), (in Russian)
A.N. Charakhchyan, G.A. Bazilevskaya, A.N. Kvashnin, T.N. Charakhchyan, Trudy FIAN, Nauka, Moscow **88**, 51 (1976b), (in Russian)
W.E. Cobb, H.J. Wells, J. Atmospheric Sci. **27**, 814 (1970)
A.H. Compton, E.O. Wollan, R.D. Bennett, Rev. Sci. Instr. **5**, 415 (1934)
D.J. Cooke, J.E. Humble, M.A. Shea et al., Nuovo Cimento C **14**, 213 (1991)
L.R. Dartnell, L. Desorgher, J.M. Ward, A.J. Coates, Biogeosciences **4**, 545 (2007)
L. Desorgher, E.O. Flückiger, M. Gurtner et al., Int. J. Modern Phys. A **20**, 6802 (2005)
G. Dobson, A comparison of the electrical conditions of the atmosphere at Kew and Eskdalemuir with notes on observations of atmospheric electricity made in other countries. Geophysical Memoirs **7**, 155–169, Meteorological Office, His Majesty's Stationery Office (1914)
L.I. Dorman, *Cosmic Rays in the Earth's Atmosphere and Underground* (Kluwer, Dordrecht, 2004)
H. Ebert, Physik Zeitschrift **2**, 662 (1901)
V.I. Ermakov, G.A. Bazilevskaya, P.E. Pokrevsky, Y.I. Stozhkov, J. Geophys. Res. **102**, 23413 (1997)
V.I. Ermakov, Y.I. Stozhkov, N.S. Svirzhevsky, in *Proc. 6th Russian Conf. Atm. Electricity*, Nizhni Novgorod (2007), p. 79 (in Russian)
J. Feynman, A. Ruzmaikin, Geophys. Res. Lett. **26**, 2057 (1999)
E.L. Fleming, S. Chandra, J.J. Barnett, M. Corney, Adv. Space Res. **10**(12), 11 (1990)
S.E. Forbush, J. Geophys. Res. **59**, 525 (1954)
H. Gerdien, Ein neuer Apparat zur Messung der elektrischen Leitfähigkeit der Luft, Nachrichten von der Gesellschaft der Wissenschaften zu Göttingen, 240 (1905)
A.E. Golenkov, A.K. Svirzhevskaya, N.S. Svirzhevsky, Y.I. Stozhkov, in *Proc. 21st Int. Cosmic Ray Conf.*, Adelaide, vol. 7 (1990), p. 14
P.K.F. Grieder, *Cosmic Rays at Earth: Researcher's Reference Manual and Data Book* (Elsevier, Amsterdam, 2001)
M. Gurtner, L. Desorgher, E.O. Flückiger, M.R. Moser, Adv. Space Res. **36**, 2176 (2005)
M. Gurtner, L. Desorgher, E.O. Flückiger, M.R. Moser, Adv. Space Res. **37**, 1759–1763 (2006)
R.G. Harrison, Surv. Geophys. **25**, 441 (2004)
R.G. Harrison, Rev. Sci. Inst. **76**, 126111 (2005)
R.G. Harrison, Atmos. Res. **84**, 182 (2007)

R.G. Harrison, A.J. Bennett, J. Atmos. Sol.-Terr. Phys. **69**, 515 (2007)
R.G. Harrison, W.J. Ingram, Atmos. Res. **76**, 49 (2004)
R.G. Harrison, D.B. Stephenson, Proc. R. Soc. A **462**, 1221 (2006)
A. Hensen, J.C.H. van der Hage, J. Geophys. Res. **99**, 10693 (1994)
V.F. Hess, Phys. Zeitschr. **13**, 1084 (1912)
J. Kazil, E.R. Lovejoy, M.C. Barth et al., Atmos. Chem. Phys. **6**, 4905 (2006)
D.R. Kniveton, J. Atmos. Sol.-Terr. Phys. **66**, 1135 (2004)
D.R. Kniveton, M. Todd, Geophys. Res. Lett. **28**, 1527 (2001)
G.A. Kovaltsov, I.G. Usoskin, Adv. Geosci. **13**, 31 (2007)
A.I. Kurguzova, T.N. Charakhchyan, Geomagn. Aeron. **23**, 715 (1983)
L.I. Miroshnichenko, *Solar Cosmic Rays* (Kluwer, Dordrecht, 2004)
D. Lario, G.M. Simnett, Solar energetic particle variations, in *Solar Variability and Its Effects on Climate*, ed. by J.M. Pap et al.. Geophys. Monograph, vol. 141 (AGU, Washington, 2004), p. 195
W.M. Lowder, P.D. Raft, H.L. Beck, in *Proc. National Symp. on Natural and Manmade Radiation in Space*, ed. by E.A. Warman (NASA, 1972), p. 908
V.S. Makhmutov, G.A. Bazilevskaya, M.B. Krainev, M. Storini, in *Proc. 27th Internat. Cosmic Ray Conf.*, Hamburg (2001), p. 4196
N. Marsh, H. Svensmark, Space Sci. Rev. **94**, 215 (2000)
K.G. McCracken, J. Beer, J. Geophys. Res. **112**, A10101 (2007)
I.A. Mironova, M.I. Pudovkin, Geomagn. Aeron. **45**, 221 (2005)
A. Mishev, P. Velinov, C.R. Acad. Bulg. Sci. **60**(5), 511 (2007)
G.J. Molina-Cuberos, J.J. Lopez-Moreno, R. Rodrigo, L.M. Lara, K. O'Brien, Planet. Space Sci. **47**, 1347 (1999)
G.J. Molina-Cuberos, W. Stumptner, H. Lammer, N.I. Kömle, K. O'Brien, Icarus **154**, 216 (2001)
H.V. Neher, W.H. Pickering, Phys. Rev. **61**(7), 407 (1942)
H.V. Neher, J. Geophys. Res. **72**, 1527 (1967)
H.V. Neher, J. Geophys. Res. **76**, 1637 (1971)
N. Nerukar, W.R. Webber, J. Geophys. Res. **69**, 815 (1964)
K. O'Brien, J. Geophys. Res. **84**, 423 (1979)
K. O'Brien, in *Proc. 7th Internat. Symp. on the Natural Radiation Environment*, ed. by J.P. McLaughlin, S.E. Simopoulos, F. Steinhusler (Elsevier, Amsterdam, 2005), p. 29
V.P. Okhlopkov, Y.I. Stozhkov, Bull. Russ. Acad. Sci. Phys. **69**, 998 (2005)
E. Pallé, C.J. Butler, K. O'Brien, J. Atmos. Sol.-Terr. Phys. **66**, 1779 (2004)
W.D. Pesnell, R.A. Goldberg, C.H. Jackman, D.L. Chenette, E.E. Gaines, J. Geophys. Res. **105**(A10), 22943 (2001)
G. Pfotzer, Z. Phys. **102**, 23 (1936)
C. Plainaki, A. Belov, E. Eroshenko et al., J. Geophys. Res. **112**, A04102 (2007)
M.I. Pudovkin, S.V. Veretenenko, J. Atmos. Terr. Phys. **57**, 1349 (1995)
M.I. Pudovkin, S.V. Veretenenko, Adv. Space Res. **17**, 161 (1996)
E. Regener, Phys. Zeitschr. **35**, 784 (1934)
V.C. Roldugin, B.A. Tinsley, J. Atmos. Sol.-Terr. Phys. **66**, 1143 (2004)
V.K. Roldugin, E.V. Vashenyuk, Geomagn. Aeron. **34**, 251 (1994)
J.M. Rosen, D.J. Hofmann, W. Gringel, J. Geophys. Res. **90**, 5876 (1985)
J.M. Rosen, D.J. Hofmann, J. Geophys. Res. **93**, 8415 (1988)
J. Schröter, B. Heber, F. Steinhilber, M.B. Kallenrode, Adv. Space Res. **37**, 1597 (2006)
J.A. Simpson, Space Sci. Rev. **93**, 11 (2000)
O.I. Shumilov, E.A. Kasatkina, K. Henriksen, E.V. Vashenyuk, Ann. Geophys. **14**, 1119 (1996)
C.M.H. Smith, *A Textbook of Nuclear Physics* (Pergamon, Oxford, 1966)
P.H. Stoker, Space Sci. Rev. **73**, 327 (1994)
Y.I. Stozhkov, J. Phys. G **29**, 913 (2003)
Y.I. Stozhkov, P.E. Pokrevskii, Z. Zullo et al., Geomagn. Aeron. **36**, 211 (1996)
Y.I. Stozhkov, N.S. Svirzhevsky, G.A. Bazilevskaya et al., *Cosmic ray investigations in the atmosphere of the Arctic and Antarctic*. Arctic and Antarctic collected papers, **3**(37), 114, Moscow, Nauka (2004), (in Russian)
Y.I. Stozhkov, N.S. Svirzhevsky, G.A. Bazilevskaya et al., *Fluxes of cosmic rays in the maximum of absorption curve in the atmosphere and at the atmosphere boundary (1957–2007)*. Lebedev Phys. Inst. Report Series, No. 14 (2007a). Online version: http://sites.lebedev.ru/DNS_FIAN/show.php?page_id=1949
Y.I. Stozhkov, V.I. Ermakov, N.S. Svirzhevsky, in *Proc. 6th Russian Conf. Atm. Electricity*, Nizhni Novgorod, (2007b), p. 198 (in Russian)
H. Svensmark, E. Friis-Christensen, J. Atmos. Sol.-Terr. Phys. **59**, 1225 (1997)
H. Svensmark, J.O.P. Pedersen, N.D. Marsh et al., Proc. Roy. Soc. **A463**, 385 (2007)

B.A. Tinsley, G.M. Brown, P.H. Scherrer, J. Geophys. Res. **94**, 14783 (1989)
B.A. Tinsley, G.W. Deen, J. Geophys. Res. **96**, 22283 (1991)
B.A. Tinsley, L. Zhou, J. Geophys. Res. **111**, D16205 (2006)
B.A. Tinsley, G.B. Burns, L. Zhou, Adv. Space Res. **40**, 1126 (2007)
I.G. Usoskin, K. Mursula, S.K. Solanki et al., J. Geophys. Res. **107**(A11), 1374 (2002)
I.G. Usoskin, O.G. Gladysheva, G.A. Kovaltsov, J. Atmos. Sol.-Terr. Phys. **66**, 1791 (2004a)
I.G. Usoskin, N. Marsh, G.A. Kovaltsov et al., Geophys. Res. Lett. **31**, L16109 (2004b)
I.G. Usoskin, K. Alanko-Huotari, G.A. Kovaltsov, K. Mursula, J. Geophys. Res. **110**, A12108 (2005)
I.G. Usoskin, G.A. Kovaltsov, J. Geophys. Res. **111**, D21206 (2006)
I.G. Usoskin, M. Voiculescu, G.A. Kovaltsov, K. Mursula, J. Atmos. Sol.-Terr. Phys. **68**, 2164 (2006)
I.G. Usoskin, S.K. Solanki, G.A. Kovaltsov, Astron. Astrophys. **471**, 301 (2007)
I.G. Usoskin, M. Korte, G.A. Kovaltsov, Geophys. Res. Lett. **35**, L05811 (2008a)
I.G. Usoskin, L. Desorgher, P. Velinov et al., Ionization of the Earth's atmosphere by solar and galactic cosmic rays. Acta Geophys. **56** (2008b, in press)
E.V. Vashenyuk, Y.V. Balabin, B.B. Gvozdevsky, S.N. Karpov, Geomagn. Aeron. **46**, 424 (2006)
P. Velinov, L. Mateev, Geomagn. Aeron. **30**, 593 (1990)
S.V. Veretenenko, M.I. Pudovkin, J. Atmos. Sol.-Terr. Phys. **59**, 1739 (1997)
S. Veretenenko, P. Thejll, J. Atmos. Sol.-Terr. Phys. **66**, 393 (2004)
M. Voiculescu, I.G. Usoskin, K. Mursula, Geophys. Res. Lett. **33**, L21802 (2006)
G.R. Wait, J. Wash. Acad. **36**, 321 (1946)
J.R. Winckler, K.A. Anderson, Phys. Rev. **108**, 148 (1957)
C.T.R. Wilson, Proc. R. Soc. Lond. A **80**, 542–537 (1908)
J.R. Wright, O.F. Smith, Phys. Rev. **7**, 49 (1916)